Table of Contents

Effect of CT Simulator Tube Voltages on CT Number and Relative Electron Density of CT Images

D P De Sliva[1]*****, A H Dilip Kumara[1], K L Priyalal[1], K L I Gunawardhana[1]

[1] Department of Radiotherapy, Cancer Unit, Teaching Hospital Karapitiya, Sri Lanka

ABSTRACT

The radiotherapy treatment planning for the cancer patient begins with the imaging of the patient using a Computed Tomography (CT) simulator. The CT simulator determines the locations and densities of patient organs using pixels. Each pixel has a unit called a CT number, or Hounsfield Unit (HU), to express the quantity of radiation attenuation in patient tissues. The density of human tissue is presented in Relative Electron Density (RED). The conversion relationship between RED and CT numbers is required to be determined and fed to the Treatment Planning System (TPS). The TPS calculates the radiotherapy dose for the patient using this CT-RED conversion curve. Most TPSs contain a single CT-RED curve defined at a specific CT tube voltage.

In this research, we studied the effect of CT tube voltages using a CT simulator (GE; CT-RED curve defined at 140kV) at Teaching Hospital Karapitiya, which provides step voltages of 80 kV, 120 kV, and 140 kV, XIO TPS, and Thorax Phantom (CIRS) containing 5 tissue types. According to the measured results, CT numbers decrease with increasing CT Tube voltage. Also, there were no significant errors in RED values of tissues at 120 kV, with respect to the 140 kV. But there were 5.55%, 2.10%, 0.99%, 0.99%, 0.95%, and 1.34% errors in RED for lung, adipose, water, T1420, muscle, and bone tissues respectively at 80kV with respect to 140 kV.

Key Words: Radiotherapy, CT imaging, CT Number, CT tube voltage, Relative Electron Density

pinsara82@gmail.com

INTRODUCTION

The determination of dose distribution within the treated volume is an essential step of modern treatment planning in radiotherapy. Many factors influence the dose distribution, and the heterogeneity of the patient's body is one of them (Parker et al., 1979). Data customization for each patient is therefore required for the dose calculations. Computed Tomography (CT) has been used as a fundamental source of such data for over 30 years now and is used as a foundation for treatment planning. Furthermore, the presentation of CT is fundamental, as it provides information on the attenuation of radiation by the patient's tissues in the form of CT numbers, expressed in Hounsfield Units (HUs) as in the following equation (Bryant et al., 2012):

$$HU_{tissue} = [(\mu_{tissue} - \mu_{water}) / \mu_{water}] \times 1{,}000 \qquad (1)$$

Where μ_{tissue} is the linear attenuation coefficient of tissue and μ_{water} is the linear attenuation coefficient of water. It is known that a precise calculation of dose distribution in radiotherapy can be performed based on the fundamental knowledge of the Relative Electron Density (RED) of the tissues. Treatment Planning Systems (TPS) usually convert HU values to RED (normalized to water) using the predefined relationship (CT to RED curve) between the two quantities (Witold et al., 2010). In some TPS, the relationship is fixed (CT-RED curve is fixed at the XiO TPS used for treatment planning of cobalt machine of Teaching Hospital Karapitiya); in others, the user can change it.

HUs for a given tissue depend on the quality of the X-ray beam; therefore, the values can differ between scanners. Even for a single scanner, CT numbers for the same tissue depend on the tube voltage. Different tube voltages are selected for CT scan imaging to obtain a quality image. As an example, if CT scans are obtained using 80 kV instead of 140 kV while using the same CT-RED relationship obtained at 140 kV, the dose calculated by TPS can be inaccurate. The CT-RED relationships can be measured during the calibration of a CT simulator with the use of body phantoms containing tissue-equivalent materials, i.e., materials that have an atomic composition similar to human tissues. The accuracy of dose distribution depends on the accuracy of the CT number and RED values that are defined by the TPS (Witold et al., 2010).

The main objective of this research work is to study the effect of CT simulator tube voltages on CT number and RED of images. Here, we have a single CT to RED curve. Since the accuracy of RED directly affects calculations of radiotherapy dose distribution the findings of this research work will be very important. Also, measuring the linear attenuation coefficient and calculating the average CT number of tissue equivalent materials for three different tube voltages are the specific objectives of this work.

INSTRUMENTATION, THEORY&METHODOLOGY

Figure 1: The GE CT Simulator (Source:https://ctmedicalscanners.com/ge-lightspeed-rt-16-ct-scanner/)

A CT (Computed-Tomography) Simulator consists of a CT scanner with a flat tabletop, a patient positioning and marking system with external lasers, CT-simulation 3D treatment planning software, and various hardcopy output devices. The CT scanner is used to acquire a volumetric CT scan of a patient, which represents the ‘‘virtual’’ or digital patient. The CT simulation software provides virtual representations of the geometric capabilities of a treatment machine (Sherouse and Chaney, 2003). This software can be a special virtual simulation program or it can be a component of a treatment planning system. Often, CT simulation is referred to as virtual simulation and the two terms tend to be used interchangeably. Virtual simulation is used to define any simulation based on software created ‘‘virtual simulator’’ and a volumetric patient scan. The following Table 1 shows the different tissue types with their density values and HU values using the Advanced Signal Processing Handbook (Stergios, 2003).

Table 1: CT numbers of Tissue Types (Stergios, 2003)

Tissue type	Density (g/cm^3)	HU
Air	0.001	-1000.0±05.0
Lung	0.300	-706.3±23.3
Adipose	0.920	-86.8±18.1
Breast	0.990	-20.3±15.1
Muscle	1.060	-21.0±10.0
Water	1.015	0±00.5
Brain	1.045	30.9±15.2
Liver	1.080	94.5±17.2
Inner bone	1.120	60.3±17.9
Bone Mineral	1.145	238.0±19.6
Cortical Bone	1.840	1273.1±19.8

The gamma-ray linear attenuation coefficient describes the absorption of gamma rays per unit length of an absorber material. This quantity depends on the energy of the incident gamma-ray beam and the density of the absorptive material. It is expressed numerically in units of m^{-1} (Ermis and Celiktas, 2012).
When a pencil gamma beam with the intensity of I_0transmits perpendicularly with an absorber of thickness x, the intensity (I) passing through the absorber can be evaluated by equation 2

$$I = I_0 e^{-\mu x} \quad (2)$$

CT measures the attenuation coefficient of an object and converts the value assigned to each voxel into a CT number, and the absorbed dose to a patient in radiation therapy is calculated using the RED of each voxel in the CT image of the patient. The correlation between the CT number and the electron density is derived from a CT scan of the materials with known RED and the points between the derived relations are filled up by interpolations. This relation is applied during the dose calculation based on the CT image and thus, the accurate measurement of CT number and applying the value to the treatment planning system (TPS) is fundamental to radiation therapy. The attenuation coefficient varies with a chosen X-ray tube voltage (kV) from the CT scanner since the attenuation coefficient has anenergy-dependent property and has discovered significant CT number changes in different kV for most materials.
The maximum difference between the real values of RED (as given by the manufacturers of the phantom) and the RED obtained by the TPS should not exceed 0.05 (Tolerance level)(Seco and Evans, 2006).
The CT simulator machine and CMS XiO TPS of Teaching Hospital Karapitiya were used to carry out this research project. All the experiments were conducted at the radiotherapy unit of Teaching Hospital Karapitiya. The CT simulator machine at Teaching Hospital Karapitiya contains a voltage generator that can be operated for 80 kV, 120 kV, 140 kV, and 10 mA to 440 mA in 5 mA increments.
CIRS (brand name) Thorax Phantom (model 002LFC) and five tissue equivalent rods were used in this experiment. Tissue-equivalent rods are removable, and they can be inserted into the holes in the CIRS phantom. Electron density relative to water is known, and a distilled water syringe was used for experiments.

Figure 2: CIRS Body Phantom

The PTW 30010 chamber and UNIDOS electrometer were selected as suitable measuring devices for the experiments. PTW 30010 chamber (sensitive volume: 0.6 cm3) responses for energy range: 30 keV–50 keV photon and electron radiation. The UNIDOS electrometer contains an accuracy of ± 0.5% ± 1 digit.

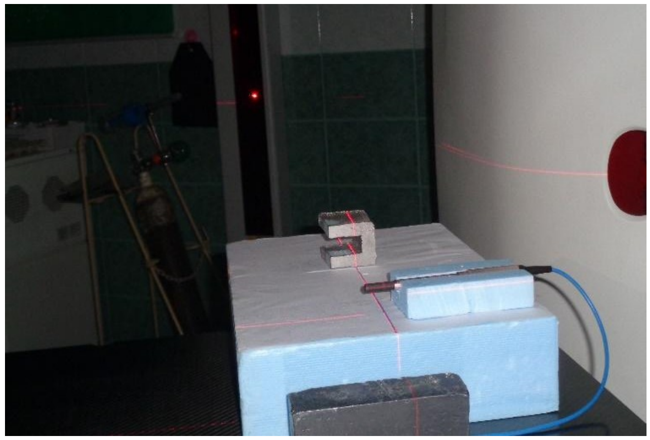

Figure 3: Experimental Setup

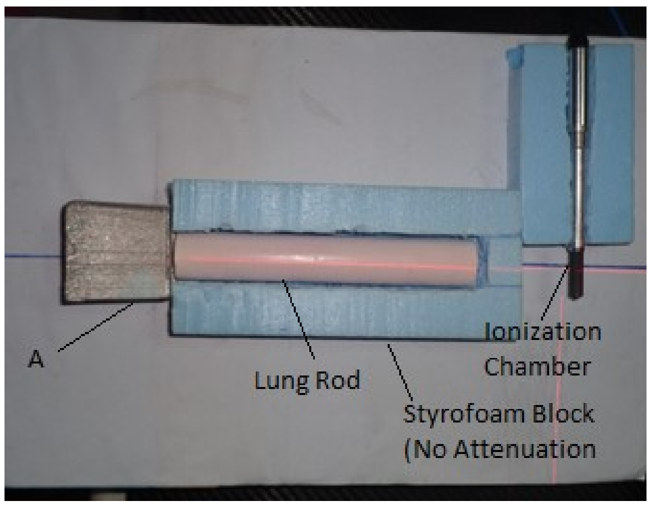

Figure 4: Experimental Setup (Lung Rod)

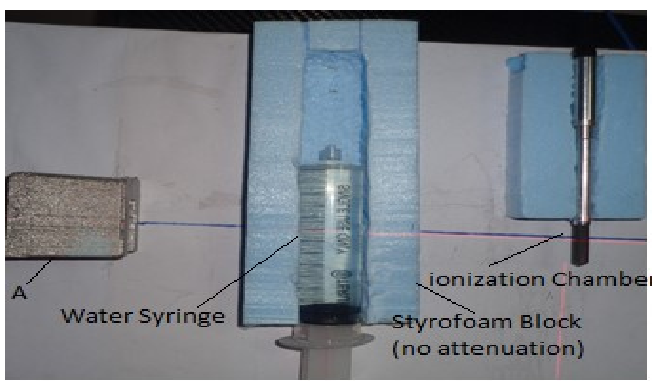

Figure 5: Experimental Setup (Water Syring)

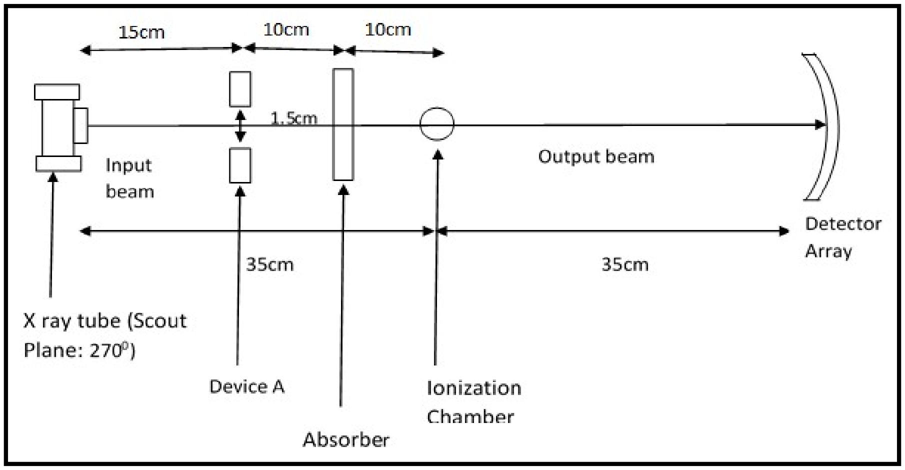

Figure 6: Experimental Setup

The experimental setup was arranged on the couch of the CT machine as above. The distance between the absorbance material and the ionization chamber, as well as the distance between the absorbance material and the X-ray head, was maintained as same. The attenuation factor of the air gap affects the measurements. The lead attenuator marked A was designed and made by using lead alloy in the mould room of Teaching Hospital Karapitiya. The purpose of the attenuator is to cut off the diverged X-ray beams and measure the narrowed X-ray beam that is perpendicular to the absorber. The isocenter of the setup (focus) was selected at the effective point (center) of the ionization chamber (Figure 3).

The study was carried out at three CT tube voltages: 80 kV, 120 kV, and 140 kV, respectively, at a constant tube current (80 mA). Five lateral X-rays (Scout plane: 270^0) were measured without an absorber for each energy level to obtain a significant reading on the electrometer. This reading was considered the incident X-ray beam intensity (Figure 3). There is no tube rotation during the scout scan process. The field length of CT scanning is defined by the longitudinal distance of couch movement.

During this research project, couch movement distance was maintained as a constant for a scout image (5 cm of couch movement within 1.9 s duration). That causes the ion chamber reading to maintain the same scatter effect during the couch (experimental setup) movement that is required to complete the scout scan process. The window of the X-ray beam attenuator (device A) is 1.5 cm x 2.0 cm, and the CT simulator produces the fan beam geometry X-ray beam output of 1mm (scan mode: 2 slices x 0.5 mm). Therefore, the cross-sectional dimension of the input X-ray beam incident on the absorber is 0.36 mm x 2.5 cm. The cross-sectional dimension of the output X-ray beam incident on the ionization chamber is 0.50 mm x 3.0 cm. The dimensions were calculated according to the divergence of the X-ray beam. Then absorbance material was kept between device A and the ionization chamber, and the output was measured by applying five lateral X-rays (Scout plane 270^0) for the above three CT tube voltage sat 80 mA (Figure 4, and Figure 5). The same couch movement distance (5 cm) and time duration (1.9 s) were maintained for all measurements.

The average absorber thickness has been changed in an appropriate way to obtain a significant electrometer reading. As an example, if a photon beam was transmitted through the 16-cm length of the bone rod, the meter reading was not sufficient to obtain due to higher attenuation. Also, at lower kV (80 kV), the meter reading was not detected even with a 5 cm absorber thickness. Correction was done to omit the attenuation of the syringe wall during the experiments conducted with water.

RESULTS AND DISCUSSION

The above setup (Figure 6) has been used to carry out the experiments, as a narrowed photon beam has been used for the experiments and the ionization chamber diameter is very low (0.61 cm) compared to the rod diameter (2.5cm). Linear attenuation coefficients of selected absorbance materials were calculated by using Equation 2. When a pencil gamma beam with an intensity of I_0 transmits perpendicularly with an absorber of thickness x, the intensity (I) passing through the absorber can be evaluated by equation 2,μ is the x-ray attenuation coefficient of the absorbent material. Then CT numbers of different absorbance materials were calculated in HU units by using equation 1 for different kV settings.

Measuring the CT number and RED of selected materials using the TPS was done by conducting experiments with the XiO TPS. All the absorbance materials were set up on the couch of the CT simulator machine, obtained CT images at corresponding energy levels, and transferred to the TPS. (Slice Thickness: 0.5 cm, Tube Current: 80 mA). During the image loading, the CT number to relative electron density conversion process has been selected. This process is performed by the radiotherapy TPS by using the predefined CT number to RED conversion curve (Figure 7) defined at 140 kV. That curve is the only curve available in this XiOTPS.

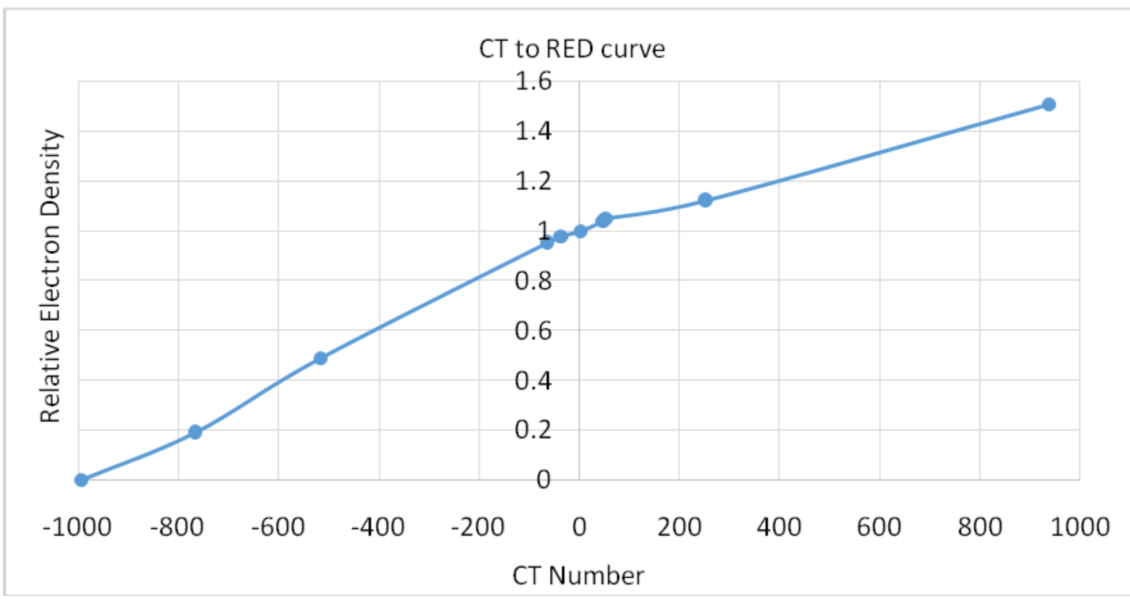

Figure 7: CT-RED curve derived in TPS defined at 140 kV

All the images were prepared as required for the planning process (similar to body outlining). The maximum value, minimum value, and mean value of CT numbers were obtained by selecting an ROI (Region of Interest).RED values were observed with the same window by following the same procedures as above.

Experimentally calculated linear attenuation coefficients and CT number values are presented in Table 2 at 80 kV, 120 kV, and 140 kV.

Table 2: Experimentally calculated linear attenuation values and CT values

Absorber Material	Density kgm^{-3}	80 kV setting		120 kV setting		140 kV setting	
		$\mu(m^{-1})$	CT valve	$\mu(m^{-1})$	CT valve	$\mu(m^{-1})$	CT valve
Water	1000	20.50	0	17.68	0	17.53	0
Lung	210	10.43	-491	4.33	-755	3.69	-789
Adipose	960	18.23	-124	16.58	-62	15.82	-97
Soft Tissue T1420	1030	21.19	33	18.17	27	17.66	7
Muscle	1060	24.39	189	18.78	62	18.66	64
Bone	1600	45.58	1223	36.18	1046	31.62	803

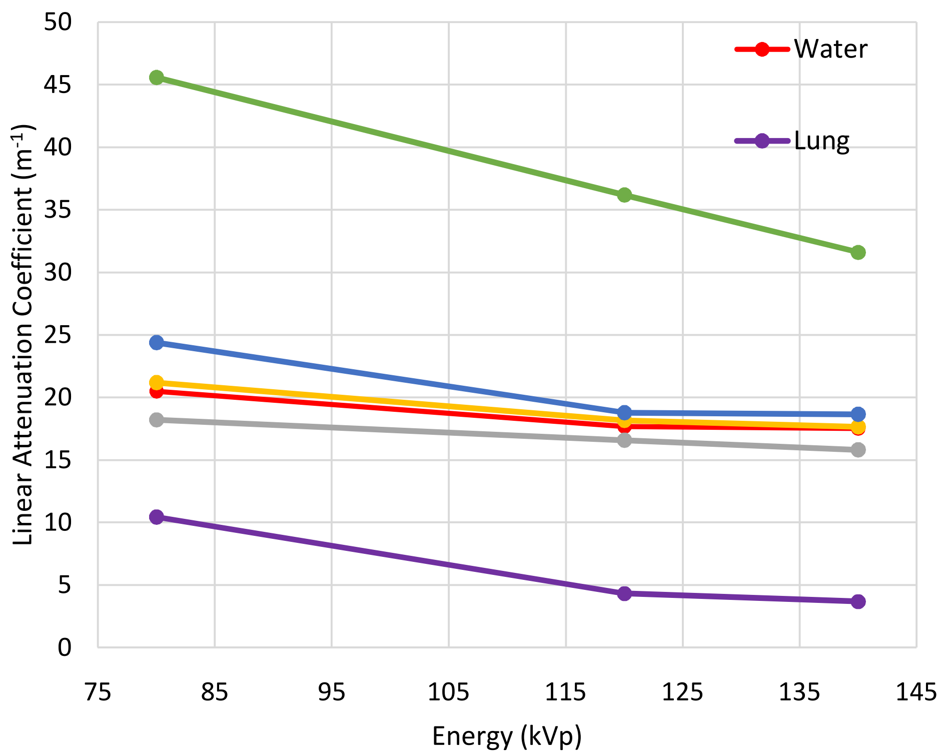

Figure 8: Variation of linear attenuation coefficient values with kV for human tissues

CT number values and RED values obtained through TPS are presented in Table 3 and Table 4.

Table 3: Average CT number values obtained by TPS

Absorber Material	80 kV, 80 mA CT value	120 kV, 80 mA CT value	140 kV, 80 mA CT value
Water	5	3	3
Lung	-620	-780	-783
Adipose	-130	-68	-58
T1420(Soft Tissue)	20	6	11
Muscle	155	140	85
Bone	1235	945	907

Table 4: Average RED values obtained by TPS

Absorber Material	RED (IAEA TECDOC 1583)	140 kV, 80 mA RED	80 kV, 80 mA RED	% error 80kV (With respect to the 140kV)	120 kV, 80 mA RED	% error 120kV (With respect to the 140kV)
Water	-	1.01	1.02	0.99%	1.01	0
Lung	0.207	0.18	0.19	5.55%	0.18	0
Adipose	0.949	0.95	0.93	2.10%	0.95	0
Soft Tissue T1420	-	1.01	1.02	0.99%	1.01	0
Muscle	1.042	1.05	1.06	0.95%	1.05	0
Bone	1.506	1.49	1.51	1.34%	1.49	0

The maximum difference between the real values of RED (as given by the manufacturers of the phantom) and the RED obtained by the TPS should not exceed 0.05 (Tolerance level)(Seco and Evans, 2006). RED values obtained by the TPS of image sets that were scanned at 140kV, 120kV, and 80kV are within the tolerance level when compared with the RED value given by the manufacturer.

DISCUSSION

Computed tomography (CT) measures the attenuation coefficient of an object and converts the value assigned to each voxel into a CT number. In radiation therapy, the CT number, which is directly proportional to the linear attenuation coefficient, is required to be converted to RED for radiation dose calculation for cancer treatment. However, if various tube voltages were applied to take the patient's CT image without applying the specific CT number to the RED conversion curve, the accuracy of the dose calculation would be unassured. In this study, changes in CT numbers for different materials due to changes in tube voltage were analyzed.

The response of normal tissues to radiation is a deterministic effect. Where, the deterministic effects (or tissue reactions) of ionizing radiation are directly related to the absorbed radiation dose, and the severity of the effect increases as the dose increases. There is a threshold (of the order of magnitude of 0.1 Gy or higher) for the deterministic effect. Below the threshold dose, the effect is not present. This radiation response follows a sigmoidal shape. The steep part of the slope indicates the region where a small deviation in dose may cause large tissue toxicity as tumor control curve and normal tissue damage curve are close together.

Radiotherapy is a compromise between a cure and an acceptable risk of complication. Acceptable risk of complications depends on risk level, organ involved, and severity of complications. The level of risk may differ between physicians and patients. Therefore, it is very important to precisely calculate and deliver the radiotherapy doses. The findings of this research work are very important to improve the accuracy of dose calculation.

In this study, three imaging kV levels (80 kV, 120 kV, and 140 kV) were considered at 80 mA for several tissue equivalent rods (bone, lung, muscle, adipose, soft tissue) of Thorax phantom (CIRS). According to the results, the linear attenuation coefficient quadratically decreases with increasing photon energy as the photoelectric effect and Compton scattering effects are dominant at these energy levels. CT number values obtained by both methods were varied with kV. According to the results, CT numbers decrease with increasing kV.

According to the results of this research work, RED values obtained by using the TPS were slightly varied with kV. The maximum differences between the observed RED values and the real values of RED (as given by the manufacturers of the phantom) were within the tolerance level (<0.05).

[

The CT to RED curve of XiO TSP is defined at 140 kV and therefore CT number to RED conversion has correctly applied for the 140 kV image set. Therefore, the 140 kV level can be considered as a reference to calculate the % error of RED at the other two kV settings. There were no considerable errors in RED values of tissues at 120 kV, with respect to the 140 kV level even though there were differences in CT numbers at those two kV setting image sets. (The difference between 120kV and 140kV tube voltages is not much larger)

But there are 5.55%, 2.10%,0.99%,0.99%,0.95%, and 1.34% errors in RED for lung, adipose, water, T1420 tissue, muscle, and bone tissues respectively at 80kV, with respect to the 140 kV level.

[

Same as this study according to Rhee et al. (2015) difference in CT number by different kVps(CT tube voltages) was considerable for most materials except for air where the density is very low and therefore noise affects the more considerably. CT x-ray tube voltage variations have considerable effects on the *RED–CT number* conversion curves. The differences between *RED–CT number* curves increase with the increase of CT x-ray tube voltage for the equivalent tissues that have densities more than water density, but below water density, the effect is negligible(Afifi et al., 2020). According to Saini et al. (2021), different kVp setting shows variation in the measured HU values. The highest variation was observed in the case of high-density bone material at the lowest kVp tube voltage.

CONCLUSION

CT number values obtained by both methods were varied with CT tube voltage. According to the results, CT numbers decrease with increasing kV.The140 kV level was considered as a reference to calculate the percentage error of RED at the other two kV settings. There were no errors in RED values of tissues at 120 kV, with respect to the 140 kV level even though there were differences in CT numbers at those two kV image sets. But there are 5.55%, 2.10%,0.99%,0.99%,0.95%, and 1.34% errors in RED for lung, adipose, water, T1420 tissue, muscle, and bone tissues respectively at 80kV, with respect to the 140 kV level. According to the study, the effect is considerable in bone and lung tissues. Therefore dose distribution calculation errors can be dominant in the chest, head and neck, and pelvic regions. It is required to determine the impact of CT tube voltage variation on radiotherapy dose calculation to ensure and enhance the radiotherapy treatment accuracy.

LIMITATIONS

There were only three kV settings available with our CT simulator machine; therefore, the study was limited to three levels. The available CIRS phantom contained just five types of human tissues, and it also didn't contain any metal inserts (high-density metal implants are inserted in patients).

RECOMMENDATIONS

A CT simulator that contains more kV settings (tube voltages) and a CIRS body phantom that has more human tissue types and metal inserts are more deserving in determiningthe impact of CT tube voltage on the CT-RED curve for further studies. According to this research work, there is an impact on CT number and RED with different tube voltages. Since radiotherapy dose calculation accuracy is very important to cure a tumour, it is required to determine the effect on dose calculation with varying imaging kV settings (CT tube voltage).

ACKNOWLEDGEMENT

Special words of thanks go to the Director of Teaching Hospital Karapitiya for giving me the approval to access the CT simulator and other facilities of Teaching Hospital Karapitiya. Also, I wish to express my gratitude to all officers and workers of the Department of Radiotherapy Teaching Hospital Karapitiya, who helped me in this task in countless ways.

REFERENCES

1. Ahnesjö, A. and Aspradakis, M.M., (1999). Dose calculations for external photon beams in radiotherapy. Physics in Medicine & Biology, 44(11), p.R99.
2. Afifi, M.B., Abdelrazek, A., Deiab, N.A., Abd El-Hafez, A.I. and El-Farrash, A.H., (2020). The effects of CT x-ray tube voltage and current variations on the relative electron density (RED) and CT number conversion curves. *Journal of Radiation Research and Applied Sciences*, *13*(1), pp.1-11.
3. Brunckhorst, E., Gershkevitsh, E., Ibbott, G., Korf, G., Miller, D. and Schmidt, R., (2008). IAEA-TECDOC-1583 Commissioning of radiotherapy treatment planning systems: testing for typical external beam treatment techniques. Vienna: International Atomic Energy Agency.
4. Bryant, J.A., Drage, N.A. and Richmond, S., (2012). CT number definition. Radiation Physics and Chemistry, 81(4), pp.358-361.

5. Camoni, L., Santos, A., Attard, M., Mada, M.O., Pietrzak, A.K., Rac, S., Rep, S., Terwinghe, C., Fragoso Costa, P. and Technologist Committee of the European Association of Nuclear Medicine (EANM), (2020). Best practice for the nuclear medicine technologist in CT-based attenuation correction and calcium score for nuclear cardiology. *European Journal of Hybrid Imaging*, *4*, pp.1-20.
6. Claude, K.P., Schandorf, C., Amuasi, J.H. and Tagoe, S.N.A., (2013). Fabrication of a tissue characterization phantom from indigenous materials for computed tomography electron density calibration: peer-reviewed original article. *South African Radiographer*, *51*(1), pp.9-17.
7. Constantinou, C., Harrington, J.C. and DeWerd, L.A., (1992). An electron density calibration phantom for CT-based treatment planning computers. Medical physics, 19(2), pp.325-327.
8. Cozzi, L., Fogliata, A., Buffa, F. and Bieri, S., (1998). Dosimetric impact of computed tomography calibration on a commercial treatment planning system for external radiation therapy. *Radiotherapy and oncology*, *48*(3), pp.335-338.
9. Du Plessis, F.C.P., Willemse, C.A., Lötter, M.G. and Goedhals, L., (2001). Comparison of the Batho, ETAR, and Monte Carlo dose calculation methods in CT-based patient models. *Medical Physics*, *28*(4), pp.582-589.
10. Ermis, E. and Celiktas, C., (2012). A Different Way to Determine the Gamma-ray Linear Attenuation Coefficients of Materials. *International Journal of Instrumentation Science*, *1*(4), pp.41-44.
11. Guan, H., Yin, F.F. and Kim, J.H., (2002). Accuracy of inhomogeneity correction in photon radiotherapy from CT scans with different settings. *Physics in Medicine & Biology*, *47*(17), p.N223.
12. Hubbell, J.H., (1996). Tables of x-ray mass attenuation coefficients and mass energy-absorption coefficients. *http://physics. nist. gov/PhysRefData/XrayMassCoef/*.
13. Jones, A.O. and Das, I.J., (2005). Comparison of inhomogeneity correction algorithms in small photon fields. *Medical physics*, *32*(3), pp.766-776.
14. Knöös, T., Nilsson, M. and Ahlgren, L., (1986). A method for conversion of Hounsfield number to electron density and prediction of macroscopic pair production cross-sections. *Radiotherapy and Oncology*, *5*(4), pp.337-345.
15. Kurudirek, M., (2014). Effective atomic numbers and electron densities of some human tissues and dosimetric materials for mean energies of various radiation sources relevant to radiotherapy and medical applications. *Radiation Physics and Chemistry*, *102*, pp.139-146.
16. Ma, C., Cao, J., Yin, Y. and Zhu, J., (2014). Radiotherapy dose calculation on KV cone-beam CT image for lung tumor using the CIRS calibration. *Thoracic Cancer*, *5*(1), pp.68-73.
17. Mohammadi, G.F., Alam, N.R., Rezaeejam, H., Pourfallah, T.A. and Zakariaee, S.S., (2015). Assessment of target volume doses in radiotherapy based on the standard and measured calibration curves. *Journal of Cancer Research and Therapeutics*, *11*(3), pp.586-591.
18. Parker, R.P., Hobday, P.A. and Cassell, K.J., (1979). The direct use of CT numbers in radiotherapy dosage calculations for inhomogeneous media. *Physics in Medicine & Biology*, *24*(4), p.802
19. Rhee, D.J., Kim, S.W., Jeong, D.H., Moon, Y.M. and Kim, J.K., (2015). Effects of the difference in tube voltage of the CT scanner on dose calculation. *Journal of the Korean Physical Society*, *67*, pp.123-128.
20. Saini, A., Pandey, V.P., Kumar, P., Singh, A. and Pasricha, R., (2021). Investigation of tube voltage dependence on CT number and its effect on dose calculation algorithms using thorax phantom in Monaco treatment planning system for external beam radiation therapy. *Journal of Medical Physics*, *46*(4), pp.315-323.

21. Saw, C.B., Loper, A., Komanduri, K., Combine, T., Huq, S. and Scicutella, C., (2005). Determination of CT-to-density conversion relationship for image-based treatment planning systems. *Medical Dosimetry*, *30*(3), pp.145-148.
22. Seco, J. and Evans, P.M., (2006). Assessing the effect of electron density in photon dose calculations. *Medical physics*, *33*(2), pp.540-552.
23. Sherouse GW, Chaney EL. The portable virtual simulator. Int J RadiatOncolBiol Phys. (1991) Jul;21(2):475-82. doi: 10.1016/0360-3016(91)90799-a. PMID: 2061124.
24. Sontag, M.R. and Cunningham, J.R., (1978). The equivalent tissue-air ratio method for making absorbed dose calculations in a heterogeneous medium. *Radiology*, *129*(3), pp.787-794.
25. Stergiopoulos, S., (2003). Advanced signal processing handbook: theory and implementation for radar, SONAR, and medical imaging real-time systems. *Medical Physics*, *30*(5), p.995
26. Yamada, S., Ueguchi, T., Ogata, T., Mizuno, H., Ogihara, R., Koizumi, M., Shimazu, T., Murase, K. and Ogawa, K., (2014). Radiotherapy treatment planning with contrast-enhanced computed tomography: feasibility of dual-energy virtual unenhanced imaging for improved dose calculations. *Radiation oncology*, *9*(1), pp.1-10.
27. Zhang, G.S., Huang, S.M., Chen, C., Xu, S.K., Zhang, D.D. and Deng, X.W., (2014). Evaluating the therapeutic dose distribution of intensity-modulated radiation therapy for head and neck with cone-beam computed tomography image: a methodological study. *BioMed research international*, *2014*.